Appl. Phys. A 66, S239–S243 (1998)

Applied Physics A
Materials
Science & Processing

Finite element simulations of the resolution in electrostatic force microscopy

S. Belaidi[1], **F. Lebon**[2], **P. Girard**[1], **G. Leveque**[1], **S. Pagano**[2]

[1] Laboratoire d'Analyse des Interfaces et de Nanophysique (UPRESA CNRS 5011),
[2] Laboratoire de Mécanique et de Génie Civil (UMR CNRS 4408), Université de Montpellier II, 34095 Montpellier Cedex 5, France
(Fax: +33-0467/521584, E-mail: girard@lain.univ-montp2.fr)

Received: 25 July 1997/Accepted: 1 October 1997

Abstract. In this paper, we present simulation results for the electrostatic force between two conducting parts placed at different voltages: an atomic force microscope (AFM) sensor and a metallic sample. The sensor is composed of a cantilever supporting a conical tip terminated by a spherical apex. The simulations are based on the finite element method. For tip–sample distances (5–50 nm) and for an electrically homogeneous plane, the electrostatic force can be compared to the results obtained with the equivalent charge model and experiment. By scanning a plane with a potential step, the variation of the electrostatic force near the discontinuity gives the spatial resolution in electrostatic force microscopy (EFM). We establish then the relationships between the resolution, tip–sample distance, and tip apex radius.

The electrostatic force microscope results from one of many specializations of tip sensor in near-field microscopy [1, 2]. More precisely, this type of microscope is realized by applying a voltage on a conducting AFM tip. It is a good tool for imaging samples that present a gradient of electrical properties [3–5]. Variations of flexion of the cantilever holding the tip during a scan allow us to construct an electrical image [6] on inhomogeneous materials as well as on nanostructures (superlattices, nanoelectronics, etc.) [7–9]. In the simple case where the tip is in front of a conductive plane sample, we can deduce the force applied on the sensor by means of analytical expressions [10–12] or an equivalent charge model [13]. As soon as the geometry of the sample becomes complex (integrated circuits, dielectrics), the theoretical behavior of the system can be obtained by numerical methods such as the surface charge method [14], finite difference method [15], or finite element method [16].

To determine the properties of the electrostatic force microscope in front of a sample with areas at different potentials, we propose to use the finite element method. In Sect. 1 we verify the results obtained by this numerical method in the simple case of a tip in front of a plane sample at constant potential [13]. In Sect. 2 we consider the response of the microscope near a potential step [17]. For this, we study the 3-dimensional tip–object system and determine the force applied on the tip by the finite element method and then we deduce the resolution for a potential step.

1 Mathematical model

1.1 The electrostatic problem

The problem consists in determining the interaction between an AFM sensor (tip + cantilever) and an infinite plane (both conducting). If the tip is long enough or the distance d between the tip and the sample is small, we can neglect the effect of the cantilever [18]. Then, the study is reduced to the calculation of the force exerted on a conical tip in front of a metallic plane. We treat the problem in 3-dimensional space because heterogeneities, as introduced in Sect. 2, cause the revolution symmetry to disappear. First, we must obtain the potential distribution in the space between the tip and the plane.

We solved the Laplace equation in a domain Ω bounded by Γ. Γ is composed of three parts Γ_0, Γ_1, and Γ_2, which are defined given potentials and electrical fields (see Fig. 1). The problem is written as follows:

$$\Delta v = 0 \text{ in } \Omega \tag{1}$$

$$v = v_0 \text{ on } \Gamma_0 \tag{2}$$

$$v = v_1 \text{ on } \Gamma_1, \text{ for a simple conducting plane} \tag{3}$$

$$\frac{\partial v}{\partial n} = 0 \text{ on } \Gamma_2 \tag{4}$$

where v_0 and v_1 are the constant applied polarizations of the tip and the sample and n the vector normal to the surface.

The domain Ω is chosen sufficiently large to neglect the edge effects and to allow us to approximate closely the prob-

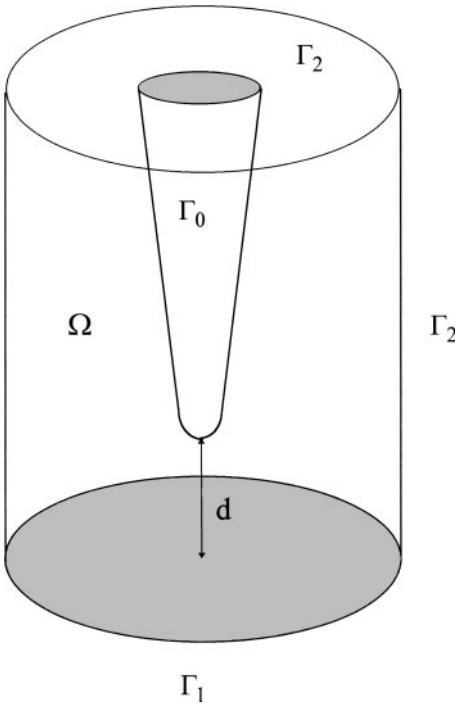

Fig. 1. Domain Ω for the finite element method with boundary conditions

lem of the single tip in front of an infinite plane in infinite space.

1.2 Application of the finite element method to obtain the potential

In order to solve numerically the problem, the domain Ω is split into tetrahedrons (or pentahedrons). On each tetrahedron, between the nodes, the potential is interpolated by a piecewise polynomial approximation of degree equal to one. The problem consists of the determination of the potential values at each node of the triangulation, i.e. the vector $[V_h]$ (h being the elementary size of the tetrahedron, in the 3-D space).

Classically, this leads to a linear system [19]

$$[A_h][V_h] = [b_h] \tag{5}$$

$[b_h]$ is a right-hand side taking into account the boundary conditions, as already defined, and $[A_h]$ is a symmetric and positive definite matrix depending on the triangulation and whose order is equal to the number of nodes N_h (N_h up to 150 000).

The solution of system (5) gives us an approximation of the potential distribution in the domain Ω, this approximation is controlled by the size h, i.e. the number of nodes [19].

1.3 Electrostatic force deduction

In the mathematical frame of the finite element method it is possible to extract the electrical field on the boundary Γ_0 from the solution given by (5).

Then, the electrostatic force F_z is given by:

$$F_z = \int_{\Gamma_0} \boldsymbol{\sigma}\boldsymbol{k}\,\mathrm{d}s \tag{6}$$

where $\boldsymbol{k}$ is the unit vector in the z direction,

$$\sigma = \frac{1}{2}\varepsilon_0 E^2 \boldsymbol{n} \quad , \quad E = \frac{\partial v_h}{\partial n} \text{ is the electrical field.} \tag{7}$$

The calculation gives also the charge distribution on the tip and the plane, which allows us to localize the part of the tip which contributes to the interaction and the area concerned on the plane.

For two typical tips, i.e. length $L = 4\,\mu\mathrm{m}$ or $10\,\mu\mathrm{m}$, apex radius $R = 10\,\mathrm{nm}$ and the cone half angle 10°, we determined the force versus tip–sample distance d. The results are reported in Fig. 2. The finite element method results appear very close to those from the equivalent charge model that have already been validated experimentally [13]. For distances d of less than 10 nm, the force difference is no more than 10%, the interaction being localized on the apex of the tip. So, the finite element method gives the same results as other methods in the case of a single tip in front of a conducting plane.

2 Mapping of potentials on a flat surface

A material with areas of different chemical natures can present potential heterogeneities on its surface. Also, dopant concentrations in semiconductors, and oxide or absorption layers imply areas of different potential on a sample. We are interested in the simple case of two materials with different

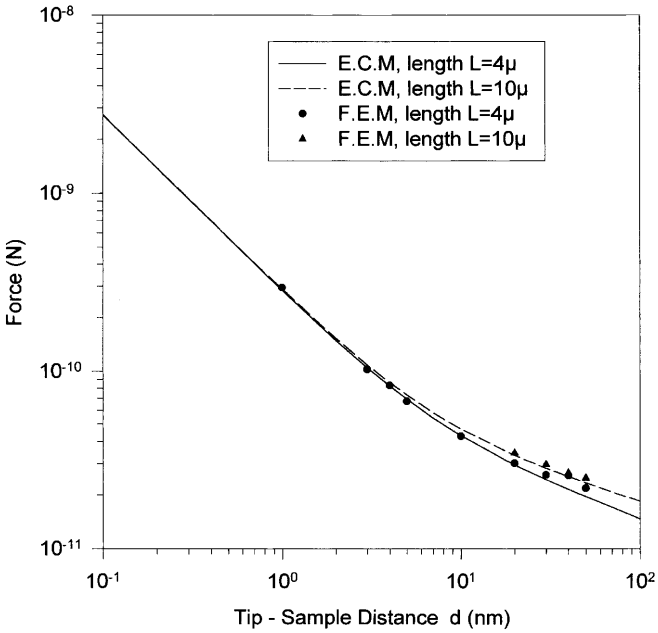

Fig. 2. Electrostatic force versus distance for two types of tips of different lengths with apex radius $R = 10\,\mathrm{nm}$ and cone half angle 10°. Comparison of results obtained by equivalent charge model (ECM) and finite element method (FEM) (1 V polarization)

work functions and we determine the response of the microscope in front of the potential step induced at the surface of the sample.

Commonly, the resolution is defined as the capability of separating two objects. For the case of a potential step on a plane sample, the concept of resolution is linked to the voltage contrast between the two areas separated by such a discontinuity. The larger the tip–sample distance is, the more the image of the discontinuity becomes blurred, the variation of the force near the frontier being weaker.

In the following, we present numerical simulation results for the voltage step and propose an analytical formulation of the resolution.

2.1 Numerical simulations

When the object is scanned at a constant height in the x direction, i.e. at right angles to the potential discontinuity, we obtain the force profiles given in Fig. 3. We ensured that we were using a sufficiently long tip. So, the effect of the cantilever is negligible and the force on the sensor is due only to the tip for distances normally used in microscopy, i.e. $d \leq 100$ nm [18].

We define here the resolution R_e as the difference between the position x_1, where the contribution to the signal is 25% of maximum, and the position x_2 where it is close to 75% of the maximum: $R_e = x_1 - x_2$ (see Fig. 3). We establish the resolution for the case of a tip at a potential of 1 V in front of a step of 0–1 V. The results are deduced from the force profile shown in Fig. 3 with a numerical uncertainty close to 2.5% (see Fig. 4). For tip–sample distances $d \geq 20$ nm, we observe that the resolution becomes dramatically weak and corresponds to the linear relation: $R_e \cong 8d$.

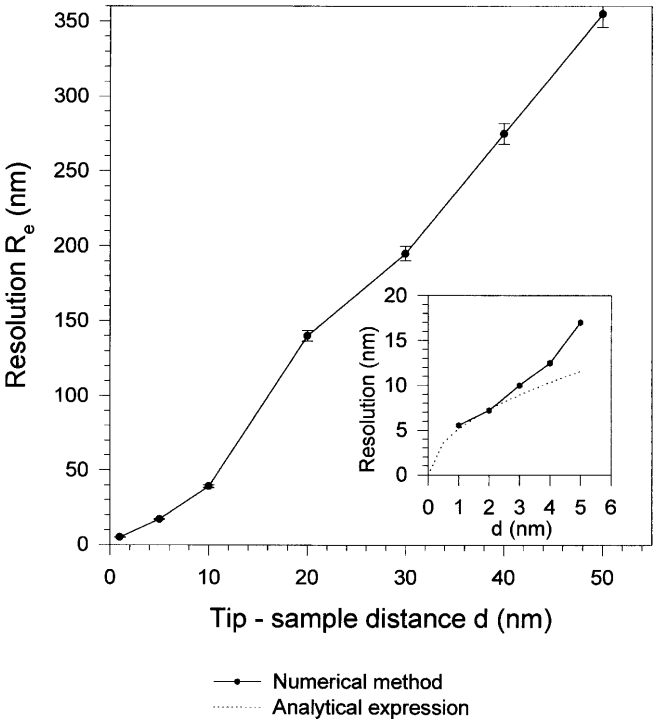

Fig. 4. Resolution versus tip–sample distance for a tip at 1 V scanning a potential step 0–1 V. Same tip as in Fig. 3

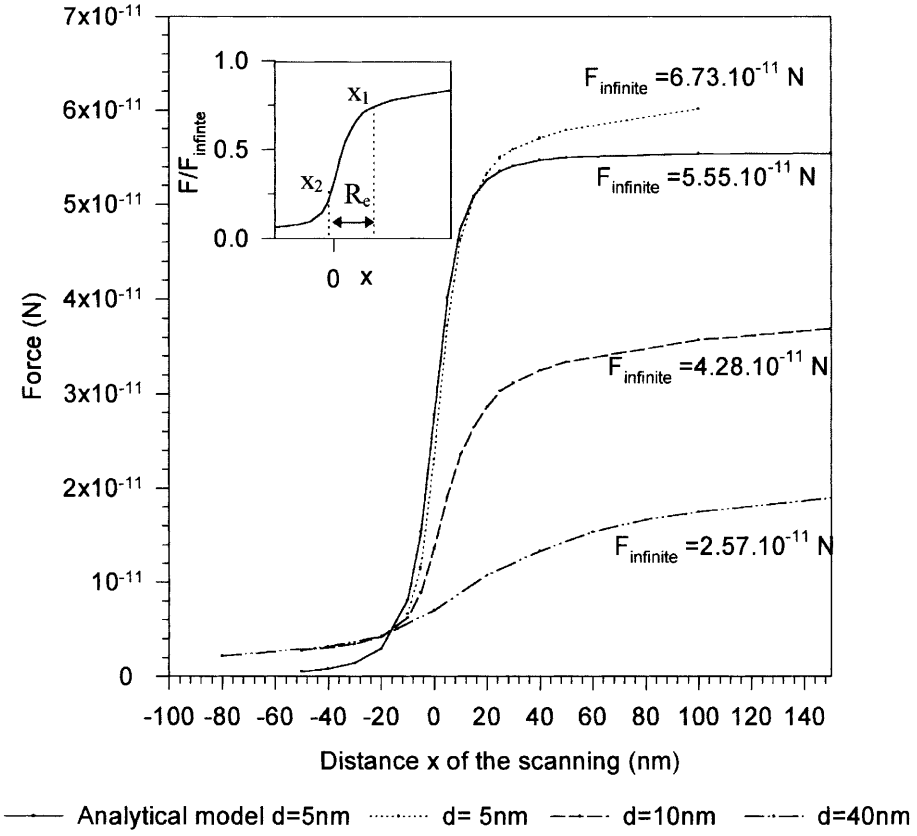

Fig. 3. Electrostatic force exerted on the tip at potential 1 V during a scanning on a potential step 0–1 V for different fixed tip–sample distances. The discontinuity is positioned at $x = 0$ and the tip length $L = 10\,\mu$m, $R = 10$ nm, and half angle is 10°

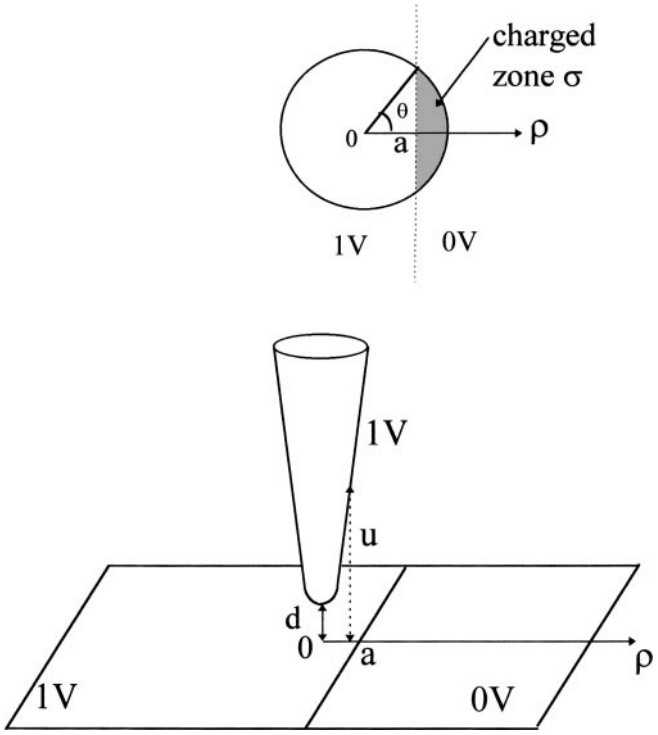

Fig. 5. Detailed representation of tip facing a potential step on a plane sample positioned at $\varrho = a$, where u is the distance used in the analytical model. Distances d and a are exaggerated for clarity. View of the charge distribution on the tip apex for this configuration

2.2 Comparison with analytical expressions

We determine below an analytical expression of the force for the system of three conductors under influence: the probe, and the two parts of the plane at potentials of 0 V and 1 V. We cannot treat the three-conductors problem. We treat separately the interaction of the tip with the different parts of the sample and neglect the effect of the frontier between two potential domains on the tip. The area of the probe at 1 V facing the surface at potential 0 V presents a charge distribution (grey area in Fig. 5). Then, we calculate the force on the tip by integrating the electrostatic pressure on its surface with the approximation of a parabolic shape for the tip. If we make the approximation of vertical electrical field lines, we can establish an analytical expression for the force for distances $d < R$ only. So, the electrical field is written as follows (see Fig. 5): $E \cong \frac{V}{u}$ where $u = d + \frac{\varrho^2}{2R}$ is the distance between a point of the tip and the plane.

We deduce the expression of the force F applied on the tip.

$$F = \iint \frac{\varepsilon_0 V^2}{2u^2}\,\mathrm{d}s \quad , \quad F = \frac{\varepsilon_0 V^2}{2} \int_{-\frac{\pi}{2}}^{\frac{\pi}{2}} \mathrm{d}\theta \int_{\frac{a}{\cos\theta}}^{\infty} \frac{\varrho\,\mathrm{d}\varrho}{\left(d + \frac{\varrho^2}{2R}\right)^2} \quad (8)$$

where a is the position of the discontinuity on the axis ϱ.

Finally, the force F is written:

$$F(a) = \frac{\pi\varepsilon_0 R V^2}{2d}\left[1 - \frac{a}{\sqrt{2Rd + a^2}}\right] \quad (9)$$

For a tip in front of a plane at constant potential ($a \to \infty$), (9) corresponds to the one obtained by the sphere model [13]. The analytical expression is plotted in Fig. 4 for a small value of distance d. At larger distances, the analytical model does not fit because real profiles are asymmetric. This occurs because the electrical field distribution at the frontier is complex: this is a horizontal component of the force. The charge distribution on the sample near the discontinuity decreases the force which reaches its maximum amplitude more slowly during the scan on the potential step. In the analytical model, the electrical field is assumed to be vertical and the effect of the discontinuity is not taken into account, so the result is symmetric.

With the criteria of Fig. 3, the analytical expression of the force (9) allows us to deduce the resolution:

$$R_\mathrm{e} = 2\sqrt{\frac{2}{3}Rd} \quad (10)$$

which agrees with the resolution deduced from the finite element method for small distances (see Fig. 4). From the study of the relationship between radius R and the distance d, we conclude that the analytical resolution is a suitable approximation for $d/R < 0.5$. This expression gives a good knowledge of image formation and allows us to deduce the transfer function and deconvolution of images. At larger distances, the finite element method is needed to predict the resolution.

3 Conclusions

We have given a numerical approach for the resolution for the problem in electrostatic force microscopy. We have shown that the resolution, for a potential step on a flat surface, depends linearly on the tip–sample distance d at large distances and varies as $d^{1/2}$ at shorter distances ($d < R/2$). The theoretical results give a resolution of about 5 nm if $d = 1$ nm. In the study of contrast formation, it will be convenient to explore also the sensitivity to step topography at constant potential and possibly separate the influences of potential and topography in the behavior of EFM.

Acknowledgements. It is a pleasure to acknowledge Mr. Gilles Requile for his helpful technical assistance. This work has been partly supported by the Centre National Universitaire Sud de Calcul (Project Lai 1005).

References

1. G. Binning, C.F. Quate, Ch. Gerber: Phys. Rev. Lett. **56**, 930 (1986)
2. Y. Martin, H.K. Wickramasinghe: Appl. Phys. Lett. **50**, 1455 (1987)
3. Y. Liang, D.A. Bonnel, W.D. Goodhue, D.D. Rathman, C.O. Bozler: Appl. Phys. Lett. **66**, 1147 (1995)
4. H. Yokoyama, T. Inoue, J. Itoh: Appl. Phys. Lett. **65**, 3143 (1994)
5. Y. Martin, D.W. Abraham, H.K. Wickramasinghe: Appl. Phys. Lett. **52** (13), 1103 (1988)
6. G. Meyer, N.M. Amer: Appl. Phys. Lett. **57**(20), 2089 (1990)
7. C. Böhm, F. Saurenbach, P. Taschner, C. Roths, E. Kubalek: J. Phys. D **26**, 1801 (1993)
8. P. Girard, G. Cohen Solal, S. Belaidi: Microelectron. Eng. **31**, 215 (1996)
9. S. Hudlet, M. Saint Jean, B. Roulet, J. Berger, C. Guthmann: J. Appl. Phys. **77**, 3308 (1995)
10. H.W. Hao, A.M. Baro, J.J. Saenz: J. Vac. Sci. Technol. B **9**, 1323 (1991)

11. H. Yokoyama, T. Inoue, J. Itoh: Appl. Phys. Lett. **65**, 3143 (1994)
12. M. Chung, N.M. Miskovsky, Paul H. Cutler, T.E. Feuctwang, E. Kazes: J. Vac. Sci. Technol. B **5**(6), 1628 (1987)
13. S. Belaidi, P. Girard, G. Leveque: J. Appl. Phys. **81**(3), 1 (1997)
14. S. Watanabe, H. Kane, T. Ohye, M. Ito, T. Got: J. Vac. Sci. Technol. B **11**, 1774 (1993)
15. U. Müller, S. Hofschen, C. Böhm, J. Sprengepiel, E. Kubalek, A. Beyer: 5th Electron and Optical Beam Testing Conference, Wuppertal, Germany, 1995, Microelectron. Eng. 31 (1996)
16. S. Lanyi, J. Török, P. Rehurek: J. Vac. Sci. Technol. B **14**(2), 892 (1996)
17. M. Nonnenmacher, M.P. O'Boyle, H.K. Wickramasinghe: Appl. Phys. Lett. **58**(25) 2921 (1991)
18. S. Belaidi, P. Girard, G. Leveque: Microel. Reliab. **37**(10–11) 1627 (1997)
19. M. Bernadou et al.: *Modulef, une bibliothéque modulaire d'éléments finis*, Ed. INRIA (1988)